

# Large-scale multiconfiguration Dirac-Fock calculations of the hyperfine-structure constants of the $2s\ ^2S_{1/2}$ , $2p\ ^2P_{1/2}$ , and $2p\ ^2P_{3/2}$ states of lithium

Jacek Bieroń,\* Per Jönsson, and Charlotte Froese Fischer

Department of Computer Science, Vanderbilt University, Nashville, Tennessee 37235

(Received 26 October 1995)

The hyperfine constants for the ground and two lowest excited states of lithium are calculated in a multiconfiguration Dirac-Fock model. Convergence of the calculated magnetic dipole and electric quadrupole constants is studied as the active set of orbitals is systematically increased. The final results are compared with experimental data and theoretical values obtained from other methods.

PACS number(s): 31.30.Gs

## I. INTRODUCTION

In the last 20 years, there has been a growing interest in the development of atomic and chemical techniques based on relativistic quantum mechanics. This interest is partially fueled by the development of experiments on highly charged ions, where storage rings or atomic traps are utilized. Calculations involving high- $Z$  species must properly account for the direct and indirect effects of relativity [1], and a four-component description becomes necessary, particularly for calculations of those atomic properties, which depend strongly on the behavior of the wave function in the proximity of the nucleus. If inner-shell electrons are involved directly in the atomic process, the magnetic and retardation effects become important, and eventually higher-order QED effects come into play with the increase of the atomic number  $Z$ .

Lithium is the simplest species in which the Pauli exclusion principle forces the electronic wave function to form two (or more) space-separated electronic shells. This feature makes lithium a natural testbed for atomic many body theories, since in very accurate calculations the electron correlation effects have to be evaluated both for the outer (valence) electron as well as within inner (core) shell itself. The objective of the present paper is to test the capacity of the new version [2,3] of the multiconfiguration Dirac-Fock (MCDF) package GRASP2 [4,5]. To facilitate the use of large configuration-state expansions, the lower triangle of the Hamiltonian matrix is stored in a sparse representation. Eigenvalues and eigenvectors are efficiently extracted by an iterative procedure [6] based on the Davidson algorithm [7].

The hyperfine interaction constants for the  $2s\ ^2S_{1/2}$ ,  $2p\ ^2P_{1/2}$ , and  $2p\ ^2P_{3/2}$  states in lithium are known to be very sensitive to the quality of the wave function, and for a long time have been a natural test case for different theoretical methods. The hyperfine constant  $A_{1/2}$  for the  $2s\ ^2S_{1/2}$  state of  $^7\text{Li}$  has been measured very accurately with the atomic-beam magnetic-resonance technique [8]. The diagonal hyperfine coupling constants for the  $2p\ ^2P_{1/2}$  and  $2p\ ^2P_{3/2}$  states have been measured in an optical double-resonance experiment

[9]. The measurements for the  $2p\ ^2P_{3/2}$  state have later been repeated with laser-induced fluorescence spectroscopy [10], and with the delayed-coincidence technique [11].

## II. THEORY

The theoretical approach employed is sketched below. A more detailed description can be found elsewhere [12–15], and only a brief résumé will be given here. Except where noted, atomic units are used in this paper.

### A. MCDF

In the MCDF method [13], the relativistic atomic state function  $\Psi$  for a state labeled  $\Gamma P J M$  is represented as a sum of symmetry-adapted configuration-state functions (CSF)

$$\Psi(\Gamma P J M) = \sum_r c_r \Phi(\gamma_r P J M). \quad (1)$$

Configuration mixing coefficients  $c_r$  are obtained through diagonalization of the Dirac Coulomb Hamiltonian

$$H_{DC} = \sum_i c \alpha_i \cdot \mathbf{p}_i + (\beta_i - 1)c^2 - Z/r_i + \sum_{i>j} 1/r_{ij}. \quad (2)$$

Configuration-state functions  $\Phi$ , which are eigenfunctions of  $J^2$ ,  $J_z$ , and parity  $P$ , are constructed as linear combinations of Slater determinants. In the restricted Dirac-Fock model a Slater determinant is a product of one-electron Dirac orbitals

$$|n \kappa m\rangle = \frac{1}{r} \begin{pmatrix} P_{n\kappa}(r) \chi_{\kappa m}(\hat{r}) \\ i Q_{n\kappa}(r) \chi_{-\kappa m}(\hat{r}) \end{pmatrix}, \quad (3)$$

where  $n$  is the principal quantum number, and  $\kappa$  and  $m$  are the relativistic angular quantum number and its  $z$  component, respectively;  $\kappa = \pm(j + \frac{1}{2})$  for  $l = j \pm \frac{1}{2}$ , with  $l$  and  $j$  being the orbital and total angular momenta of the electron.  $P_{n\kappa}(r)$  and  $Q_{n\kappa}(r)$  are the large and small component one-electron radial wave functions, and  $\chi_{\kappa m}(\hat{r})$  is the spinor spherical harmonic in the  $l s j$  coupling scheme

\*Permanent address: Instytut Fizyki, Uniwersytet Jagielloński, Reymonta 4, 30-059 Kraków, Poland.

$$\begin{aligned}\chi_{km}(\hat{r}) &= \chi_{km}(\theta, \varphi, \sigma) \\ &= \sum_{m_s} \langle lm - m_s \frac{1}{2} m_s | l \frac{1}{2} j m \rangle Y_{lm - m_s}(\theta, \varphi) \xi_{m_s}(\sigma). \quad (4)\end{aligned}$$

The radial functions  $P_{n\kappa}(r)$  and  $Q_{n\kappa}(r)$  are obtained as a self-consistent-field solution of the one-electron Dirac-Fock equation [13].

### B. Hyperfine interaction

The hyperfine structure of atomic energy levels (hereafter abbreviated hfs) is caused by the interaction between the electrons and the electromagnetic multipole moments of the nucleus. Combined with measured hfs splittings, accurate calculations of the electronic part of the interaction provide an interesting tool for determining nuclear moments. This is especially important for quadrupole moments, which are difficult to measure with direct nuclear techniques [16]. In cases where reliable values of the nuclear moments are available, it is possible to test atomic theory by comparing observed hyperfine structures with theoretically calculated ones. Theoretical studies of the hyperfine interaction have led to significant improvements in our understanding of atomic structure [12] in general, and have helped establish the applicability and limitations of different computational methods designed to account for correlation effects, the leading corrections to the independent particle model. In accurate calculations of hyperfine structures it is necessary to take relativistic effects into account even for relatively light elements [17,18]. The effects of relativity scale as the square of the atomic number  $Z$  and can usually be treated as perturbations for light elements. These effects become important with increasing atomic number, and, at some point, it becomes necessary to employ a fully relativistic approach if accurate results are to be expected [19]. This necessity is more pronounced in calculations of hyperfine structures than other atomic properties, because the hyperfine interaction is sensitive to the form of the calculated electronic wave functions close to the nucleus, where direct and indirect effects of relativity [1] are difficult to account for by quasirelativistic methods.

The hyperfine contribution to the Hamiltonian can be represented by a multipole expansion

$$H_{\text{hfs}} = \sum_{k \geq 1} \mathbf{T}^{(k)} \cdot \mathbf{M}^{(k)}, \quad (5)$$

where  $\mathbf{T}^{(k)}$  and  $\mathbf{M}^{(k)}$  are spherical tensor operators of rank  $k$  in the electronic and nuclear space, respectively [20]. The  $k=1$  term represents the magnetic-dipole interaction and the  $k=2$  term the electric quadrupole interaction. Higher-order terms are much smaller and can often be neglected.

The electronic tensor operators are sums of one-particle tensor operators

$$\mathbf{T}^{(k)} = \sum_{j=1}^N \mathbf{t}^{(k)}(j), \quad k = 1, 2. \quad (6)$$

The magnetic-dipole operator  $\mathbf{t}^{(1)}$  in nonrelativistic framework takes the form [20]

$$\begin{aligned}\mathbf{t}^{(1)} &= \frac{\alpha^2}{2} \sum_{i=1}^N \{ 2\mathbf{1}^{(1)}(i) r_i^{-3} + g_s \frac{8}{3} \pi \delta(\mathbf{r}_i) \mathbf{s}^{(1)}(i) \\ &\quad - g_s \sqrt{10} [\mathbf{C}^{(2)}(i) \times \mathbf{s}^{(1)}(i)]^{(1)} r_i^{-3} \}. \quad (7)\end{aligned}$$

The three terms in the equation (7) are usually called the *orbital*, *Fermi-contact*, and *spin-dipole* terms, respectively. In relativistic formulation the magnetic-dipole operator is more compact [20],

$$\mathbf{t}^{(1)} = -i\alpha (\boldsymbol{\alpha} \cdot \mathbf{1} \mathbf{C}^{(1)}) r^{-2}. \quad (8)$$

The electric quadrupole term has a common form in both the relativistic and nonrelativistic formulation

$$\mathbf{t}^{(2)} = -\mathbf{C}^{(2)} r^{-3}. \quad (9)$$

In the formulas above  $\alpha$  is the fine-structure constant,  $\boldsymbol{\alpha}$  is the vector of the three Dirac matrices, and  $\mathbf{C}^{(k)}$  is a spherical tensor with the components related to the spherical harmonics as

$$C_q^{(k)} = \sqrt{\frac{4\pi}{2k+1}} Y_{kq}. \quad (10)$$

The reader is referred to our previous paper [15] for the evaluation of the matrix elements of the hyperfine interaction in the framework of symmetry adapted configuration-state functions.

### C. Multiconfiguration expansion

The configuration expansions were obtained with the active space method in which configuration-state functions of a particular parity and symmetry are generated by substitutions from reference configuration to an active set of orbitals. The active set is then increased systematically until the convergence of the hyperfine constant is obtained. For smaller orbital sets employed in this study, the complete active space (CAS) method was used, in which all electrons are subject to substitutions within a particular active set. For larger orbital sets the complete active space becomes prohibitively expensive and certain limitations were needed to keep the number of configuration-state functions below the limit acceptable by the computer memory constraints. This was accomplished by (1) restricting the electron substitutions to single and double for the orbitals with high values of principal quantum number and by (2) excluding CSFs with weights smaller than a certain threshold value. The effects of these restrictions were later evaluated by separate configuration-interaction calculations. The actual sets employed are presented in Tables I, III, and IV. All single, double, and triple substitutions have been allowed to all orbitals with principal quantum numbers  $n=2,3,4,5$ . For  $n=6$  only *s,p,d,f,g* symmetries have been permitted; the *h* and higher symmetries have been excluded. Starting with  $n=7$  only single and double substitutions were permitted and the set of orbital symmetries was systematically decreased until there were only *s* orbitals (14*s*, 15*s*) added to the list.

TABLE I. Diagonal magnetic-dipole hyperfine structure parameter  $A$  (in MHz) for the  $1s^2 2s^2 S_{1/2}$  state of  ${}^7\text{Li}$  as a function of the increasing active set of orbitals. SDT means single, double, and triple substitutions from the reference  $1s^2 2s$  configuration. The SDT substitutions to  $6s5p4d3f2g$  orbital set are carried over to all subsequent larger orbital sets. Column 3 gives the number of configurations.

Active set	Type	NCF	$A_{1/2}$
DF	SDT	1	289.216
$2s1p$	SDT	8	286.443
$3s2p1d$	SDT	79	390.475
$4s3p2d1f$	SDT	410	390.652
$5s4p3d2f1g$	SDT	1463	401.822
$6s5p4d3f2g$	SDT	2739	397.186
$7s6p5d4f3g$	SD	3102	401.291
$8s7p6d5f3g$	SD	3377	400.508
$9s8p7d6f3g$	SD	3285	400.892
$10s9p8d6f3g$	SD	3975	400.555
$11s10p9d6f3g$	SD	4282	401.166
$12s11p9d6f3g$	SD	4480	401.159
$13s12p9d6f3g$	SD	4613	401.204
$14s12p9d6f3g$	SD	4762	401.202
$15s12p9d6f3g$	SD	4834	401.204
CI1		7017	401.309
CI2		11789	401.305
Breit			401.336
Nuclear recoil			401.249
QED			401.714

### III. RESULTS

The value of the nuclear magnetic-dipole moment has been adopted from the tables of Raghavan [21]. The nuclear electric quadrupole moment has been taken from the paper of Diercksen *et al.* [22]. The conversion from atomic units to MHz used the factor of 1 a.u. = 6 579 683 900 MHz.

#### A. $2s^2 S_{1/2}$ state

Table I and Fig. 1 present the magnetic dipole constant  $A$  for the ground state of lithium as a function of configuration-space expansion. Figure 1 shows that 15 energy-optimized layers of orbitals were required to converge the  $A$  value. As discussed in Sec. II C, the computational resources at our disposal did not allow us to include all configuration-state functions arising from the orbital sets and substitutions presented in Table I. The initial calculations have been performed on a SUN SparcStation, where we were forced to keep the number of CSFs below 3500, to avoid disk swapping. To overcome this limitation we employed a condensing procedure, which eliminates those configuration-state functions, which contribute to the total wave function less than a specified threshold value. Condensing was applied at the  $n=6$  level with the threshold = 0.000 000 1. The effect on the hfs occurred at the seventh decimal digit after condensing. Similar condensing was further applied at the  $n=8$  and  $n=9$  levels, where an IBM RISC 6000 workstation was used, and the disk swapping limit was 4500. The calculations for the largest expansions were performed on a Cray Y-MP, with no limits other than CPU quota. The condensing procedure has to be very carefully executed, since the last layers of orbitals contribute appreciably more to hfs than to energy.

As the next step, we evaluated the effect of the configurations, which were excluded from the CSF lists due to con-

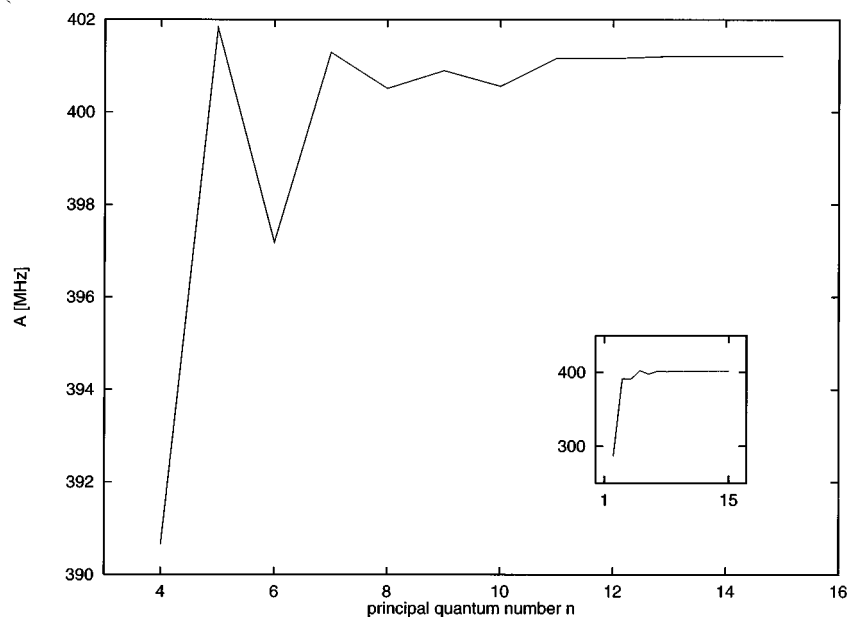


FIG. 1. Magnetic-dipole constant (in MHz) for the  $1s^2 2s^2 S_{1/2}$  state of  ${}^7\text{Li}$  as a function of orbital set. The main figure shows the blown-up tail portion corresponding to these orbital sets, for which principal quantum number of virtual orbitals is allowed to exceed 4. The inset shows the full picture.

TABLE II. Effect of the Breit interaction on the calculated diagonal magnetic-dipole hyperfine structure parameter  $A$  (in MHz) for the  $1s^2 2s^2 S_{1/2}$  state of  ${}^7_3\text{Li}$  as a function of configuration expansion. Column 1 gives the wave function composition threshold values and column 2 the number of configurations that survived the condensing procedure.

Threshold	NCF	MCDF	MCDF+Breit	Correction	Factor
0.001	69	394.040	394.104	0.064	1.0001634
0.0001	451	401.137	401.169	0.032	1.0000798
0.00001	1453	401.588	401.619	0.031	1.0000772
		extrapolated			1.0000769

densing or restrictions imposed on the allowed substitutions. To evaluate the effect of configurations resulting from triple substitutions to orbitals with high principal quantum numbers it would be desirable to do a full configuration interaction calculation in a CAS manner, i.e., with all single, double, and triple substitutions into the full orbital set. The number of configuration-state functions for such a case amounts to 39911, and it would be extremely expensive, even on a highly powerful system. We decided to perform a stepwise procedure, where subsequent CI calculations are done with expanding list of configuration-state functions. Such a procedure is not only less expensive with regard to the CPU but also provides an estimate of the precision of the CI results. The CI1 entry in Table I was obtained by a configuration-interaction calculation, where (1) all single, double, and triple substitutions to the set  $1s, 2s, 2p, \dots, 6s, 6p, 6d, 7s, 8s, \dots, 14s, 15s$  were allowed and (2) all single and double substitutions to the full active set were allowed (no condensing).

The CI2 entry was obtained by a configuration-interaction calculation, where (1) all single, double, and triple substitutions to the set  $1s, 2s, 2p, \dots, 7d, 7f, 7g$  were allowed, (2) all single, double, and triple substitutions to the set  $1s, 2s, 2p, \dots, 6d, 6f, 6g, 7s, 8s, \dots, 14s, 15s$  were allowed, and (3) all single and double substitutions to the full active set were allowed (no condensing). The difference between the results of the two CI calculations appeared at sixth figure, so we refrained from extending the CSF list further. These results also suggest that the triple substitutions involving orbitals of  $s$  symmetry with high principal quantum numbers are mainly responsible for the difference between our converged “scf” value of hfs constant  $A$  and the CI value. The difference between the two CI calculations also provides an estimate of the precision of our calculated hfs value within the model employed in this study.

The three leading corrections to the CI value arise from the nuclear motion effects, the Breit interaction, and the QED effects. The Breit contribution is very difficult to calculate in the direct calculation, even as a perturbation, due to the extremely high CPU cost. The effect of the Breit interaction on the calculated hfs constants has been estimated from a series of CI calculations performed with the full orbital set but condensed down to a small number of CSFs. The Breit interaction has been treated as a perturbation to the Coulomb Hamiltonian. The effect on the calculated hfs value is presented in Table II as a function of the size of the CI expansion. It has to be mentioned here, that the condensing procedure is based on Coulomb-only Hamiltonian matrix. Since angular properties of the Breit operator are different than

those of the Coulomb energy operator, it is important that the CI expansion arising from the condensing described above is sufficiently large to include all important contributions. As can be seen in Table II the MCDF hfs value is almost fully recovered in the largest CI calculation and the Breit contribution has saturated. The resulting Breit correction has been obtained by employing the factor extrapolated from Table II.

The nuclear motion correction was evaluated by adding the normal mass shift (NMS) and specific mass shift (SMS) operators [23] to the Hamiltonian (2) and performing a series of configuration-interaction calculations similar to those for Breit interaction, i.e., by monitoring the correction to hfs from SMS and NMS when configuration expansion was increasing.

In the next step we tested the effect of leading QED effects. Our present code allows a post-scf evaluation of second-order vacuum polarization and an estimate of the

TABLE III. Diagonal magnetic-dipole hyperfine structure parameter  $A$  (in MHz) for the  $1s^2 2p^2 P_{1/2}$  state of  ${}^7_3\text{Li}$  as a function of the increasing active set of orbitals. SDT means single, double, and triple substitutions from the reference  $1s^2 2p$  configuration. The SDT substitutions to  $6s 5p 4d 3f 2g$  orbital set are carried over to all subsequent larger orbital sets. Column 3 gives the number of configurations.

Active set	Type	NCF	$A_{1/2}$
DF	SDT	1	32.359
$2s 1p$	SDT	6	42.047
$3s 2p 1d$	SDT	76	42.334
$4s 3p 2d 1f$	SDT	403	46.725
$5s 4p 3d 2f 1g$	SDT	1454	45.948
$6s 5p 4d 3f 2g$	SDT	3697	46.065
$7s 6p 5d 4f 3g$	SD	4171	46.014
$8s 7p 6d 5f 3g$	SD	4662	45.892
$9s 8p 7d 6f 3g$	SD	5237	45.961
$10s 9p 8d 6f 3g$	SD	5111	45.967
$11s 10p 9d 6f 3g$	SD	4203	45.937
$12s 11p 9d 6f 3g$	SD	4233	45.965
$13s 12p 9d 6f 3g$	SD	4583	45.942
$14s 12p 9d 6f 3g$	SD	4300	45.943
$15s 12p 9d 6f 3g$	SD	4412	45.950
CI1		8102	45.955
CI2		12605	45.955
Breit			45.951
Nuclear recoil			45.956
QED			45.989

self-energy operator added to the Dirac-Coulomb-Breit Hamiltonian [24]. These are the two leading lowest-order QED terms in the expansion in powers of  $Z\alpha$ , and for the system as light as neutral lithium the only two that could play a significant role. After the Hamiltonian is diagonalized the effect of vacuum polarization on hfs comes through the wave function composition. The self-energy operator is evaluated as a contribution to the eigenenergies only. The combined effect of these two corrections on the total energy is of the order of 0.001%, which is consistent with the results obtained by other workers [25,26]. The effect of vacuum polarization has been found to have negligible effect on the calculated hyperfine constant, beyond the numerical precision of our code. The only non-negligible QED correction arises from the anomalous magnetic moment of the electron, for which the factor  $g_s/2 = 1.001\,159\,652\,193$  has been used [27].

The accuracy of the calculated hfs constant is of the order of 0.01%. The precision of the calculation is limited by several factors. There are several effects not accounted for by the current model, which are negligible at our present level of accuracy, but would have to be accounted for, especially when heavier nuclei are involved. The Breit interaction effect on radial wave functions becomes important for the orbitals penetrating the proximity of heavy nuclei [28]. The dipole distribution inside the nucleus due to nuclear structure (the Bohr-Weisskopf correction [29]) may be expected to affect

TABLE IV. Diagonal magnetic-dipole hyperfine structure parameter  $A$  and electric quadrupole parameter  $B$  (in MHz) for the  $1s^2 2p^2 \ ^2P_{3/2}$  state of  $^7\text{Li}$  as a function of the increasing active set of orbitals. SDT means single, double, and triple substitutions from the reference  $1s^2 2p$  configuration. The SDT substitutions to  $6s5p4d3f2g$  orbital set are carried over to all subsequent larger orbital sets. Column 3 gives the number of configurations. The electric quadrupole constants have been calculated using the semiexperimental value of nuclear quadrupole moment  $Q = -0.040\,55$  mb from Refs. [32,22].

Active set	Type	NCF	$A_{3/2}$	$B_{3/2}$
DF	SDT	1	6.4700	-0.22321
$2s1p$	SDT	8	-3.2089	-0.22401
$3s2p1d$	SDT	110	-0.0842	-0.18197
$4s3p2d1f$	SDT	645	-4.8560	-0.20925
$5s4p3d2f1g$	SDT	2478	-2.9822	-0.23478
$6s5p4d3f2g$	SDT	4181	-3.4256	-0.19591
$7s6p5d4f3g$	SDT	4994	-2.9329	-0.23538
$7s6p5d4f3g$	SD	3482	-2.9329	-0.23538
$8s7p6d5f3g$	SD	4076	-3.2309	-0.20106
$9s8p7d6f3g$	SD	4871	-3.0687	-0.22065
$10s9p8d6f3g$	SD	5078	-3.0840	-0.21147
$11s10p9d6f3g$	SD	5005	-3.0750	-0.21915
$12s11p9d6f3g$	SD	4221	-3.1005	-0.21915
$13s12p9d6f3g$	SD	4721	-3.0858	-0.21916
$14s12p9d6f3g$	SD	4268	-3.0913	-0.21916
$15s12p9d6f3g$	SD	4416	-3.0868	-0.21916
CI1		12883	-3.0771	-0.21903
Breit			-3.0771	-0.21902
Nuclear recoil			-3.0844	-0.21900
QED			-3.1060	-0.21900

the *Fermi-contact* term of the hfs, as compared to the point-dipole model. Bohr and Weisskopf estimate that this effect would lower the  $A$  value of the hfs of the  $2s \ ^2S_{1/2}$  state by about 0.01% in the extreme situation where spin and orbital nuclear magnetic moments are aligned [29]. The effect increases with  $Z$  approximately as  $Z^{4/3}$  and certainly would have to be considered for heavy nuclei [29,30]. We believe that the largest error in our calculation comes from the contributions of virtual orbitals neglected in our configuration expansions, particularly those with higher symmetries. The effect of omitted orbitals on the calculated hfs constant was evaluated by Tong *et al.* [31] by performing an  $l$  extrapolation. Since the correction arising from the extrapolation is very small and its dependence on relativistic effects is negligible, we assume that the  $l$  extrapolation in the relativistic framework would yield a similar value. If we add the estimated contribution from neglected orbitals to our final value, then the 401.765 MHz result for hyperfine magnetic-dipole constant  $A$  is obtained. This value is in very good agreement with the experimental result  $A = 401.752\,043$  MHz obtained with the atomic-beam magnetic-resonance method [8].

### B. $2p \ ^2P_{1/2}$ state

The calculations for this level were done using a similar approach to those for  $^2S_{1/2}$ . Table III presents the configuration sets employed in MCDF steps. The configuration expansions generated for the two CI calculations used exactly the same scheme as described in Sec. III A. The actual expansions are slightly larger due to a different symmetry of the reference configuration. Our Breit value of hyperfine constant  $A$  has been evaluated by scaling the mass-corrected  $A$  value by a Breit factor obtained in a procedure similar to that for the  $^2S_{1/2}$  state. The Breit factor for the  $^2P_{1/2}$  state was equal to 0.999 923 62. The nuclear motion corrections were estimated in the same way as before. The final result was obtained by employing the electron anomalous magnetic moment correction. The procedure for this correction has to be modified to account for the fact, that for the  $p$  symmetry the hyperfine Hamiltonian involves the *orbital* interaction between the magnetic moment generated by the *orbital* motion of the electronic cloud and the nucleus. In the nonrelativistic framework this corresponds to the *orbital* term in the hyperfine Hamiltonian (7). For these states for which there is nonzero *orbital* term the QED correction is obtained by multiplying the *spin-dipolar* and *Fermi-contact* terms with a factor  $g_s/2$ , but not the *orbital* term. The relativistic hyperfine Hamiltonian (8) does not separate out the *orbital* term. The correction can be entered by simply ignoring this, when the *orbital* term is expected to be small. Owing to the fact that the nonrelativistic calculations for lithium have already been performed, we applied the QED correction calculated in nonrelativistic framework. The relative difference between the two above approaches amounts to 0.1% for the  $2p \ ^2P_{1/2}$  state in lithium.

Table III and Fig. 2 present the calculated value of hyperfine constant  $A$  for the  $2p \ ^2P_{1/2}$  state, compared with other theoretical, as well as experimental results. With one exception, all theoretical values are larger than the experimental value of Orth *et al.* [9] and are one to four standard deviations outside their quoted error bar. This may be either coin-

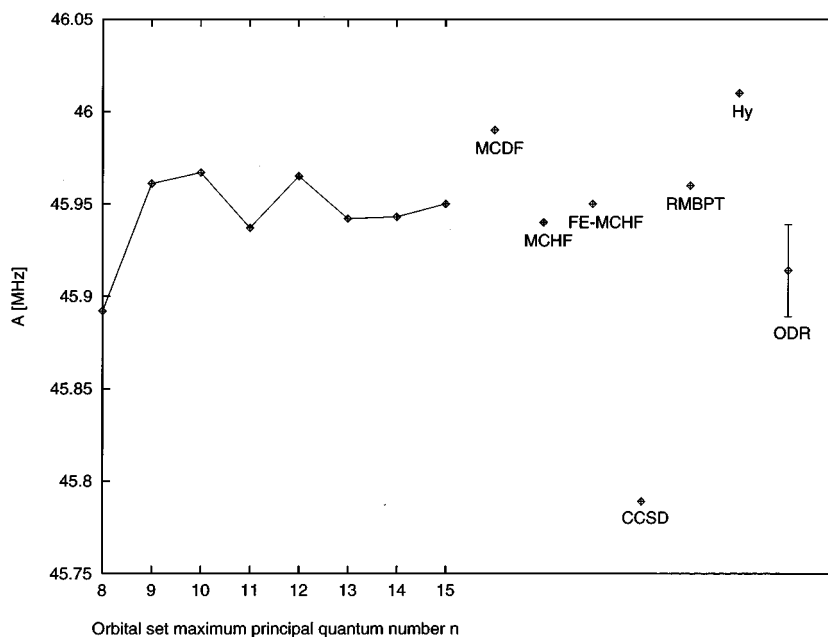


FIG. 2. Magnetic-dipole constant  $A$  (in MHz) for the  $1s^2 2p^2 P_{1/2}$  state of  ${}^7\text{Li}$ . The curve on the left-hand side shows the calculated, uncorrected value of  $A$  as a function of orbital set. The point labeled MCDF represents the result of the present calculations corrected for Breit, nuclear recoil, and QED effects; MCHF — calculation by Carlsson *et al.* [14]; FE-MCHF — finite-element MCHF calculation by Sundholm and Olsen [16]; CCSD — coupled-cluster calculation by Mårtensson-Pendrill and Ynnerman [33]; RMBPT — relativistic many-body perturbation calculation by Blundell *et al.* [34]; Hy — Hylleraas calculation by Ahlenius and Larsson [35]; ODR — optical double-resonance experiment by Orth *et al.* [9].

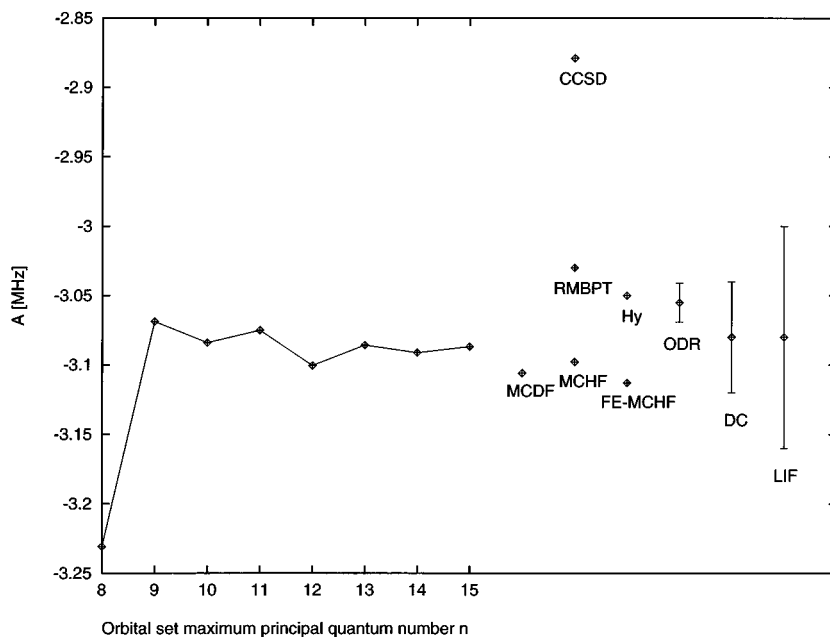


FIG. 3. Magnetic-dipole constant  $A$  (in MHz) for the  $1s^2 2p^2 P_{3/2}$  state of  ${}^7\text{Li}$ . The curve on the left-hand side shows the calculated, uncorrected value of  $A$  as a function of orbital set. The point labeled MCDF represents the result of the present calculations corrected for Breit, nuclear recoil, and QED effects; MCHF — calculation by Carlsson *et al.* [14]; FE-MCHF — finite-element MCHF calculation by Sundholm and Olsen [16]; CCSD — coupled-cluster calculation by Mårtensson-Pendrill and Ynnerman [33]; RMBPT — relativistic many-body perturbation calculation by Blundell *et al.* [34]; Hy — Hylleraas calculation by Ahlenius and Larsson [35]; ODR — optical double-resonance spectroscopy by Orth *et al.* [9]; DC — delayed-coincidence spectroscopy by Shimizu *et al.* [10]; LIF — laser-induced fluorescence spectroscopy by Carlsson and Sturesson [11].

TABLE V. Diagonal magnetic-dipole hyperfine structure constants  $A$  (in MHz) for the  $1s^2 2s^2 2S_{1/2}$ ,  $1s^2 2p^2 2P_{1/2}$ , and  $1s^2 2p^2 2P_{3/2}$  states and electric quadrupole constant  $B$  (in MHz) for the  $1s^2 2p^2 2P_{3/2}$  state of  ${}^7_3\text{Li}$ .

Method	$A$			$B$	Reference
	${}^2S_{1/2}$	${}^2P_{1/2}$	${}^2P_{3/2}$	${}^2P_{3/2}$	
MCDF	401.71	45.99	-3.106	-0.2190	This work
MCHF	401.71	45.94	-3.098	-0.2148	Ref.[14]
MCHF	401.76				Ref.[31]
FE-MCHF	401.60	45.95	-3.113	-0.2146	Ref.[16]
CCSD	400.903	45.789	-2.879	-0.2160	Ref.[33]
RMBPT	402.47	45.96	-3.03	-0.2162	Ref.[34]
Hylleraas		46.01	-3.05	-0.1921	Ref.[35]
Hylleraas	401.79 <sup>a</sup>				Ref.[36]
Hylleraas	401.89 <sup>a</sup>				Ref.[37]
Experiment	401.752043				Ref. [8]
Experiment		45.914(25)	-3.055(14)	-0.221(29)	Ref. [9]
Experiment			-3.08(4)		Ref.[10]
Experiment			-3.08(8)		Ref.[11]

<sup>a</sup>Not corrected for relativistic effects.

cidental or an artifact, but it is tempting to conclude that a new experiment would be desirable for  $2p^2 2P_{1/2}$  state of  ${}^7_3\text{Li}$ .

### C. $2p^2 2P_{3/2}$ state

We slightly simplified the calculations for the  ${}^2P_{3/2}$  level, as compared to those described in Secs. III A and III B. The MCDF calculations for the  ${}^2P_{3/2}$  level were carried out in the exactly similar manner as those for the  ${}^2P_{1/2}$ , but we performed only one final configuration-interaction (CI) calculation. This simplification was based on the observation, that the CI1/CI2 difference appeared in the sixth digit for both  ${}^2S_{1/2}$  and  ${}^2P_{1/2}$  states, while the experimental accuracy of  ${}^2P_{3/2}$  hfs constant  $A$  is in the third digit. The configuration expansion generated for the CI1 calculation amounted to 12 883 CSFs, and that for CI2 calculation would become very expensive computationally. The nuclear recoil and Breit corrections were estimated in the same way as before, and the multiplicative Breit factor for the magnetic dipole hyperfine constant  $A$  was equal to 1.000 000 2, while that for the electric quadrupole constant  $B$  was equal to 0.999 967 7. The QED correction for the hyperfine constant  $A$  for the  ${}^2P_{3/2}$  state has been evaluated in the same manner as that for  ${}^2P_{1/2}$ , by employing the correction calculated in nonrelativistic formalism.

Table IV and Fig. 3 present the calculated value of hyperfine constant  $A$  for the  $2p^2 2P_{3/2}$  state, compared with other theoretical, as well as experimental results. With one exception, all theoretical results land within the error bars quoted by the two most recent experiments [10,11], but the three variational calculations are below (and well outside the error bars of) the experimental value of Orth *et al.* [9].

A possible explanation for the low values from the variational calculations is the neglected effects from orbitals with high  $l$  quantum numbers. The importance of these orbitals is best seen in the nonrelativistic formulation. If the neglected orbitals with high  $l$  quantum numbers are taken into account, the contribution to the hyperfine constant from the *orbital*

term will increase. For the  ${}^2P_{3/2}$  state such an increase can have large effect due to the strong cancellation between *orbital* and *Fermi-contact* terms. In addition, the absence of the orbitals with high  $l$  quantum numbers increases the contributions from configurations containing orbitals with low  $l$  quantum numbers, which in effect overestimates the *Fermi-contact* term.

The last column in Table IV presents the calculated value for electric quadrupole hyperfine constant  $B$  for the  $2p^2 2P_{3/2}$  state. It has converged very well and it appears to be in very good agreement with the semiexperimental value of the nuclear quadrupole moment  $Q = -0.040 55$  mb from Refs. [32,22], but the accuracy of the experimental value of  $B$  is too low to draw any definite conclusion.

## IV. CONCLUSIONS

We have calculated the magnetic-dipole hyperfine constants  $A$  for the three lowest states of lithium and the electric quadrupole constant  $B$  for the  $2p^2 2P_{3/2}$  state. They are compared with available experimental and theoretical data in Table V. The agreement between our calculation and experiment for the hyperfine constant  $A$  of the ground state of lithium is at the 0.01% level. When  $l$ -extrapolation correction is employed the agreement comes close to 0.003%. The agreement with experiment indicates that the MCDF limit has been obtained, and further progress is limited by the precision of the determination of magnetic, retardation, radiative, and nuclear size effects. The method seems to be promising for studying QED and nuclear effects in high- $Z$  systems.

## ACKNOWLEDGMENTS

Many thanks are extended from one of us (J.B.) to Andreas Stathopoulos for his comments and for discussions on the spectral properties of large matrices, and to Anders Ynnerman for his assistance during the course of this experiment. This research was supported by the Division of Chemical Sciences, Office of Basic Energy Sciences, Office of Energy Research, U. S. Department of Energy.

- [1] The direct and indirect effects of relativity were first observed by D. F. Mayers, *Proc. R. Soc. London Ser. A* **241**, 93 (1957); for references to subsequent studies of these effects and an overview, see P. Pyykkö, *Chem. Rev.* **88**, 563 (1988).
- [2] J. Bieroń and C. Froese Fischer (unpublished).
- [3] F. A. Parpia, C. Froese Fischer, and I. P. Grant (unpublished).
- [4] F. A. Parpia, I. P. Grant, and C. Froese Fischer (unpublished).
- [5] K. G. Dylla, I. P. Grant, C. T. Johnson, F. A. Parpia, and E. P. Plummer, *Comput. Phys. Commun.* **55**, 425 (1989).
- [6] A. Stathopoulos and C. Froese Fischer, *Comput. Phys. Commun.* **79**, 1 (1994).
- [7] E. R. Davidson, *Comput. Phys.* **7**, 519 (1993); *Comput. Phys. Commun.* **53**, 49 (1989); *J. Comput. Phys.* **17**, 87 (1975).
- [8] A. Beckmann, K. D. Böklen, and D. Elke, *Z. Phys. A* **270**, 173 (1974).
- [9] H. Orth, H. Ackermann, and E. W. Otten, *Z. Phys. A* **273**, 221 (1975).
- [10] F. Shimizu, K. Shimizu, Y. Gomi, and H. Takuma, *Phys. Rev. A* **35**, 3149 (1987).
- [11] J. Carlsson and L. Sturesson, *Z. Phys. D* **14**, 281 (1989).
- [12] I. Lindgren, *Rep. Prog. Phys.* **47**, 345 (1984).
- [13] I. P. Grant, in *Relativistic Effects in Atoms and Molecules*, edited by S. Wilson, *Methods in Computational Chemistry*, Vol. 2 (Plenum Press, New York, 1988), pp. 1–71.
- [14] J. Carlsson, P. Jönsson, and C. Froese Fischer, *Phys. Rev. A* **46**, 2420 (1992).
- [15] J. Bieroń, F. A. Parpia, C. Froese Fischer, and P. Jönsson, *Phys. Rev. A* **51**, 4603 (1995).
- [16] D. Sundholm and J. Olsen, *Phys. Rev. A* **42**, 2614 (1990).
- [17] A. Rosén and I. Lindgren, *Phys. Scr.* **6**, 109 (1972).
- [18] P. Jönsson, *Phys. Scr.* **48**, 678 (1993).
- [19] J. R. Bieroń and J. Migdalek, *J. Phys. B* **25**, 4099 (1992).
- [20] I. Lindgren and A. Rosén, *Case Stud. At. Phys.* **4**, 93 (1974).
- [21] P. Raghavan, *At. Data Nucl. Data Tables* **42**, 189 (1989).
- [22] G. H. F. Diercksen, A. J. Sadlej, D. Sundholm, and P. Pyykkö, *Chem. Phys. Lett.* **143**, 163 (1988).
- [23] F. A. Parpia, M. Tong, and C. Froese Fischer, *Phys. Rev. A* **46**, 3717 (1992).
- [24] B. J. McKenzie, I. P. Grant, and P. H. Norrington, *Comput. Phys. Commun.* **21**, 233 (1980).
- [25] P. Indelicato and J.-P. Desclaux, *Phys. Rev. A* **42**, 5139 (1990), and references therein.
- [26] D. K. McKenzie and G. W. F. Drake, *Phys. Rev. A* **44**, R6973 (1991).
- [27] *CRC Handbook of Chemistry and Physics*, edited by D. R. Lide (CRC Press, Boca Raton, Florida, 1994).
- [28] P. Indelicato, O. Gorceix, and J.-P. Desclaux, *J. Phys. B* **20**, 651 (1987); E. Lindroth, A.-M. Mårtensson-Pendrill, A. Ynnerman, and P. Öster, *ibid.* **22**, 2447 (1989); H. M. Quiney, I. P. Grant, and S. Wilson, *ibid.* **23**, L271 (1990).
- [29] A. Bohr and F. Weisskopf, *Phys. Rev.* **77**, 94 (1950).
- [30] A.-M. Mårtensson-Pendrill, *Phys. Rev. Lett.* **74**, 2184 (1995).
- [31] M. Tong, P. Jönsson, and C. Froese Fischer, *Phys. Scr.* **48**, 446 (1993).
- [32] D. Sundholm, P. Pyykkö, L. Laaksonen, and A. J. Sadlej, *Chem. Phys. Lett.* **112**, 1 (1984).
- [33] A.-M. Mårtensson-Pendrill and A. Ynnerman, *Phys. Scr.* **41**, 329 (1990).
- [34] S. A. Blundell, W. R. Johnson, Z. W. Liu, and J. Sapirstein, *Phys. Rev. A* **40**, 2233 (1989).
- [35] T. Ahlenius and S. Larsson, *Phys. Rev. A* **18**, 1329 (1978).
- [36] F. W. King, *Phys. Rev. A* **40**, 1735 (1989), and references therein.
- [37] F. W. King and M. P. Bergsbaken, *J. Chem. Phys.* **93**, 2570 (1990).